

Degradation and bioactivity studies of Mg membranes for dental surgery

H. Hornberger^{a,*}, B. Striegl^a, M. Trahanofsky^a, F. Kneissl^a, M. Kronseder^b

^a Faculty Mechanical Engineering, University of Applied Science OTH Regensburg, Germany

^b Physical Department, University of Regensburg, Germany

ARTICLE INFO

Article history:

Received 22 January 2019

Received in revised form 18 March 2019

Accepted 26 March 2019

Available online 11 April 2019

Keywords:

Magnesium

Dental membrane

Bioactivity

Corrosion rate

ABSTRACT

Bioresorbable materials are under investigation due to their promising properties for applications as implant material. This study is about the degradation and bioactivity behaviour of magnesium foils, which allegorize dental membranes. The degradation behaviour including pitting corrosion during immersion tests can be precisely observed using micro-computed tomography. Using the bioactivity test according to Kokubo, it is shown that magnesium has strong Ca-phosphate layer formation correlated with high degradation. Therefore, magnesium foils appear to hold a great potential for bone implant application.

© 2019 The Authors. Published by Elsevier B.V. This is an open access article under the CC BY-NC-ND license (<http://creativecommons.org/licenses/by-nc-nd/4.0/>).

1. Introduction

The application of dental membranes, used in bone reproduction processes, is a standard procedure in the area of dental implant and periodontal surgery. Those membranes are introduced as a barrier to separate cell types like osteoblasts, which have slow proliferation, from epithelial layer and connective tissue, which show rapid proliferation. Conventional resorbable products are mostly collagen membranes applied to stabilize defect tissue, to support and guide the formation of bone. However, the mechanical stability of collagen membranes is very low. Besides their mechanical properties dental membranes are distinguished by thickness between 0.1 and 0.5 mm. Still there are controversial studies about their appropriate thickness, load sharing capacity, best composition – therefore also including the question of biocompatibility – and whether porosity is needed or not [1–3].

The initiation of this study was the product idea of degradable magnesium foils as new applications devices in oral and facial surgery because of their high mechanical stability compared to collagen. Magnesium based materials are one of the most promising biodegradable metals for implant surgery [4–7]. The requirements for resorbable dental membranes are biocompatibility, bioactivity, cavity creation or preservation and usability during implantation. This study aimed to evaluate degradation and bioactivity behavior of magnesium foils.

2. Experimental methods

Mg foils (99.9%, Goodfellow) were used in this study to allegorize dental membranes. Prior testing the samples were cleaned in ethanol. Corrosion tests were carried out in 0.9 ma% NaCl solution: one foil for 28 (Mgf17), two foils for 52 (Mgf15 and Mgf16) and two foils for 72 h (Mgf1, Mgf4). The foils showed a diameter of 8 and a thickness of 0.1 mm. The volume loss before and after corrosion test was determined by micro-computed tomography (μ -CT). Using volume loss data the corrosion rates were determined.

The bioactivity study was performed on larger foils (\varnothing 10 mm, thickness 0.25 mm) to allow the polishing of the surface, which will be in contact with simulated body fluid (SBF). Embedded in inert epoxy material, samples were treated with SiC 800, 1200 and 2400 using ethanol based solution. For the bioactivity study the SBF according to Kokubo [8] was produced, the amount of SBF V_{SBF} needed for the test was calculated according to:

$$V_{\text{SBF}}[\text{ml}] = \frac{V_{\text{sample}}[\text{mm}^3]}{10}$$

Thereby V_{sample} is the volume of the embedded sample. In this study the amount of SBF varied between 150 and 200 ml depending on the embedded sample's height. The processed surface was placed vertically in SBF to avoid simple accumulation of segregated components. The entire test build-up was stored in an incubator at 36.5 °C for 24 h for samples used in the X-ray photoelectron spectroscopy (XPS), respectively 96 h for samples analyzed via μ -CT and Fourier-transformed-infrared (FTIR) spectroscopy.

* Corresponding author.

E-mail address: helga.hornberger@oth-regensburg.de (H. Hornberger).

The change of surface morphology caused by bioactivity test was observed using laser scanning microscopy (LSM) Olympus LEXT OLS4000.

Surface layer composition before and after the bioactivity test was determined by XPS PHI 5700 XPS/ESCA. FTIR studies were performed on Thermo Scientific Nicolet iS10 FTIR and iN5 microscope spectrometer (settings: range $4000 - 650 \text{ cm}^{-1}$, 64 scans, resolution 4 cm^{-1}). The attenuated total reflection technique was applied.

The magnesium foils before and after immersion were studied using μ -CT. All scans were performed on the system phoenix v|tome|x s 240/180 research edition from GE Sensing & Inspection Technologies GmbH, software phoenix datos|x 2 acquisition 2.4.0. Scanning parameters were as follows: 50 kV voltage, 240 μ A

current, 1000 ms time, 2000 images, voxel size $12 \mu\text{m}$. Reconstructed volumes were processed using software phoenix datos|x 2 reconstruction 2.4.0. The threshold value defining the material and background was set to 0.16 absorption coefficient. 3D images and surface area and volume parameters were determined using software Volume Graphics VG Studio Max 2.2.3.

3. Results

Using μ -CT macroscopic changes in morphology and volume of the samples were observed. The whole foils could be visualized after conducting the reconstructions. Fig. 1 shows 3D models and surface morphology of the NaCl-treated magnesium foils before and after immersion tests. Localized corrosion with a large amount

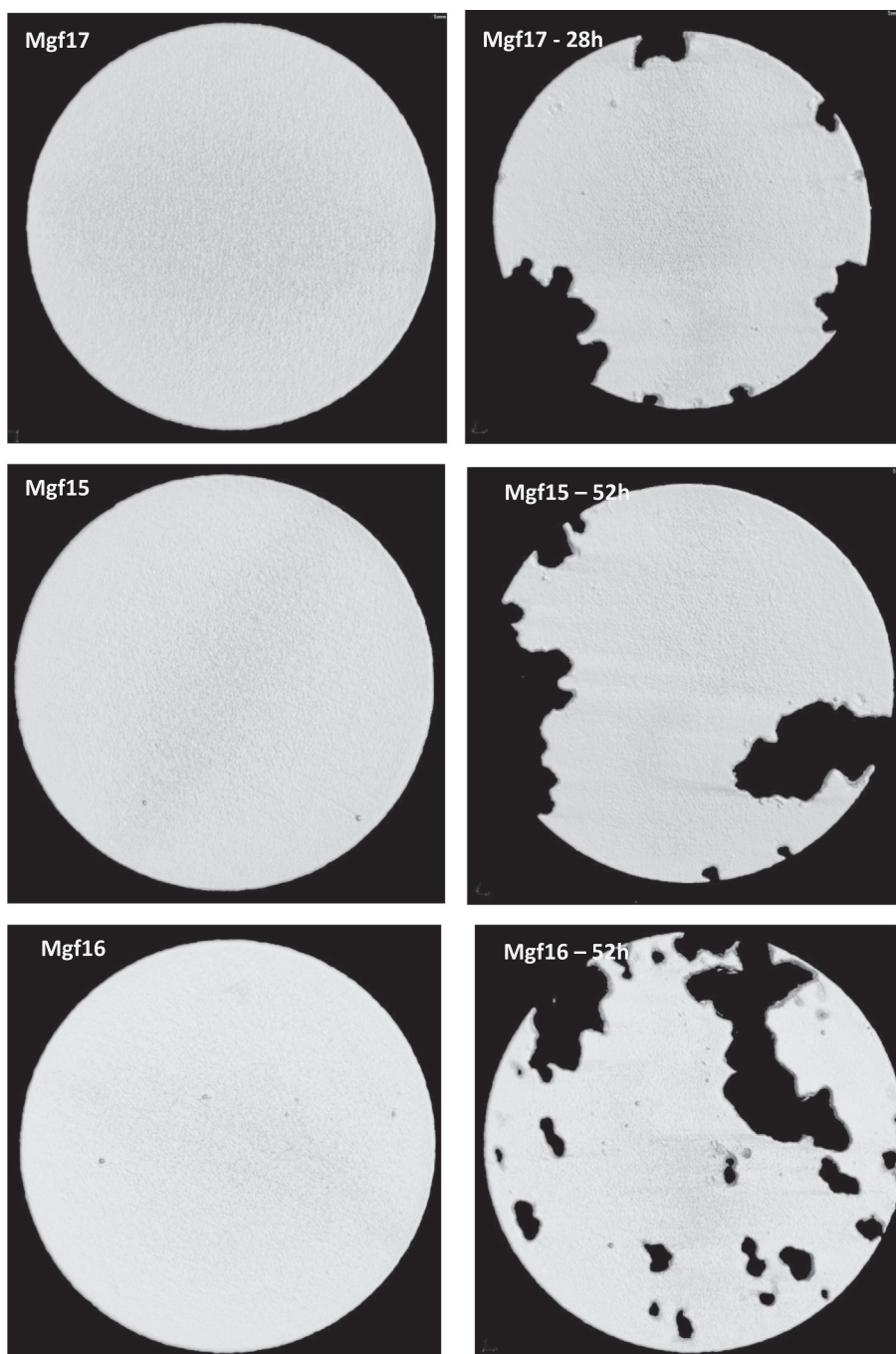


Fig. 1. Micro-CT 3D reconstruction images of NaCl-solution treated Mg foils before (left) and after (right) immersion.

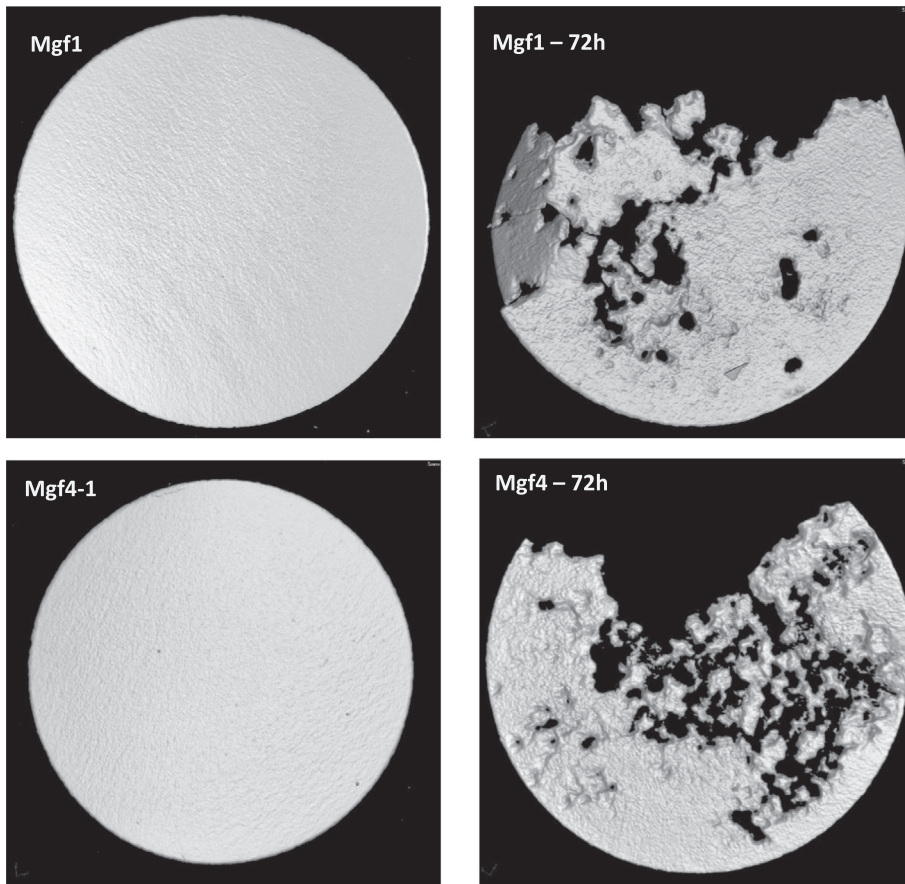


Fig. 1 (continued)

Table 1
Volume and surface area values and calculated CR for NaCl-solution treated Mg foils.

NaCl-treated-Mg sample number	Mgf17 before immersion	Mgf17 after immersion	Mgf15 before immersion	Mgf15 after immersion	Mgf16 before immersion	Mgf16 after immersion	Mgf1 before immersion	Mgf1 after immersion	Mgf4 before immersion	Mgf4 after immersion
Volume V [mm ³]	4.8	4.4	4.7	4.0	5.1	4.4	5.2	3.5	5.2	3.4
Surface S [mm ²]	100.5	94.7	100.7	85.6	101.0	88.7	104.2	71.2	103.9	75.0
S/V [1/mm]	21.0	21.4	21.5	21.6	19.8	20.3	19.9	20.5	19.8	22.5
Time [h]		28		52		52		72		72
ΔV [mm ³]	0.4		0.7		0.7		1.7		1.8	
CR [mm/year]	1.2		1.2		1.2		2.0		2.1	

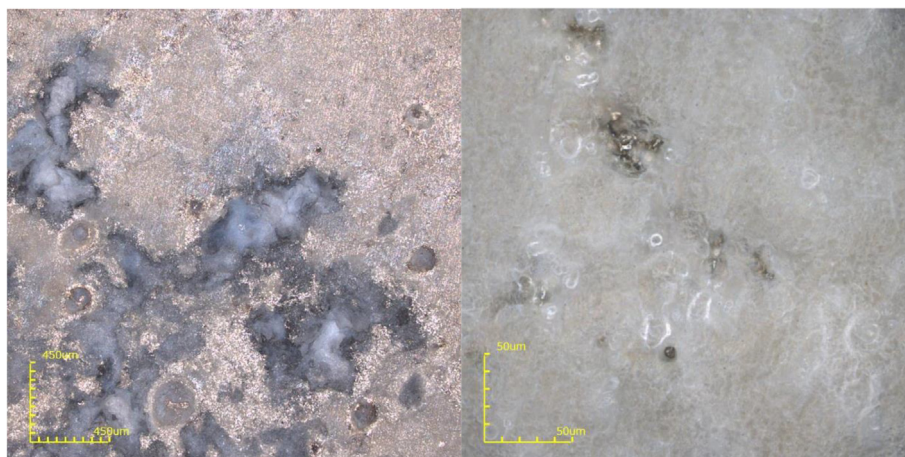


Fig. 2. LSM of foil surface after immersion in SBF for 24 h, left an overview, right some details at higher magnification.

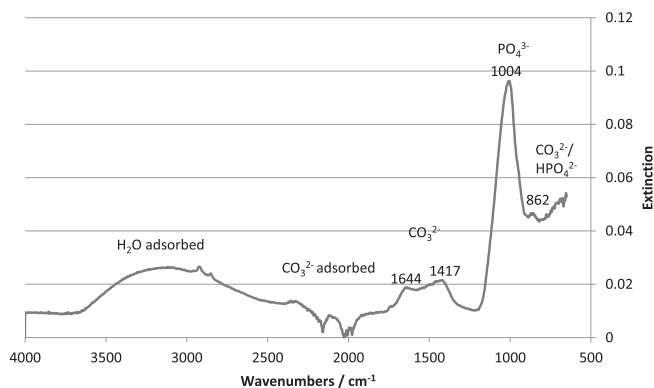


Fig. 3. FTIR spectra of the Ca-phosphate layer, which has formed on the Mg foil after immersion in SBF.

of cracks was observed on Mgf16, Mgf1 and Mgf4 after immersion tests of 52 and 72 h whereas Mgf15 and Mgf17 treated for 52 and 28 h show only flanking of the surface edge. The corrosion products are likely magnesium oxide and hydroxide.

The corrosion rates (CR) depending on the reduction of the magnesium volume after immersion tests were calculated from the obtained 3D:

$$CR = \Delta V / (A \cdot t)$$

where A is the initial foil surface area exposed to corrosion and t is the exposure time, ΔV is the reduction in volume that is equal to the remaining foil volume after immersion test subtracted from the initial volume. Table 1 shows the values of the volume and surface area reduction of the foils and the corrosion rates analyzed using μ -CT. The corrosion rates for the NaCl-treated-Mg samples are constant at 1.2 mm/year with soaking times of 28 and 52 h and then increase to 2 mm/year. The increase is caused by the loss of large pieces during 72 h as shown in Fig. 1. Using the volume μ -CT data and the density of magnesium (1.738 g/cm³) the mass loss of magnesium could be determined.

Using SBF for 24 and 96 h immersion tests, the foil surfaces showed strong layer formation observed by LSM (Fig. 2). A correlation between layer thickness and proceeding degradation (24 and 96 h) on one hand, and immersion time on the other was clearly evidenced by visual examination. XPS measurements indicated that the grown layer is composed of Ca-phosphate. FTIR spectra of the layer is shown in Fig. 3. The strongest peak at 1004 cm⁻¹ results from stretching vibrations of PO₄³⁻-ions. The weak peak at 862 cm⁻¹ can arise from HPO₄²⁻-ions or CO₃²⁻-ions. Compared to the spectra of other studies [10,11], the IR peak values for PO₄³⁻-ions and CO₃²⁻-ions are similar. But the sharp peak at 3570 cm⁻¹ of OH⁻-stretching vibrations does not occur. So it can be assumed that lattice OH⁻-ions like in natural hydroxyapatite are missing, and that only traces of CO₃²⁻-ions are incorporated into the calcium phosphate structure.

4. Discussion and conclusion

Determination of corrosion rates was challenging for fine structures like membranes because advanced pitting corrosion took place. The application of μ -CT was found to be a precise method to evaluate the volume loss of metallic magnesium. The corrosion rate of 1.2 mm/year appears for application as dental membranes nearly appropriate considering the short range of time for bone formation of about 3 months, although the applied immersion test was very simple. Furthermore, the degradation rates found *in vivo* were usually slower compared to the rates determined

in vitro [9,12]. Control of the degradation behaviour of magnesium based implants is known to be important [4,13,14]. Successful control implies that the implant will be mechanically stable after implantation as long as needed for remodelling but on the other side the complete degradation of the implant is supposed to take place in a determined time period. Negative effects by pitting behaviour or sudden pH increase can be reduced by appropriate alloying and surface modifications [15–17].

The applied bioactivity test according to Kokubo implies that all materials, which have built up a layer of apatite during the test *in vitro*, are able to bond to bone tissue *in vivo*. The observed layer growth in SBF on magnesium foils was remarkably high. XPS and FTIR measurements detected Ca-phosphate enriched with carbonate within the layer but it was not possible to conclude whether there is crystalline apatite or not. In any case it might be difficult to detect small amounts or irregular structures as it is typical for bone like apatite. Furthermore, magnesium shows high resorbability, and structures like β -tricalcium phosphate and natural calcite do not form apatite on their surfaces in SBF but they bond to living bone which could be related to their high resorbability [8]. Bioactivity of an Mg-Ca-alloy was reported by Idris et al. [18], apatite formation was only indicated by scanning electron microscopy and energy dispersive X-ray spectroscopy. Bioactivity means, that bone formation will be initiated onto the implant surface and proceed in direction of the bone. Due to high bioactivity the dental membranes made of magnesium would not need the common grid structure of conventional metallic membranes to activate bone growth. Pitting corrosion behaviour and increasing porosity during degradation process may enforce the bone formation even more, as it is well known, that biomaterials become interesting for bone formation by appropriate porosity. The results demonstrate that during SBF-immersion the build-up of a Ca-phosphate layer took place parallel to the degradation process of magnesium. The extent of degradation suppression by reaction products in the formed Ca-phosphate layer is unclear and has to be addressed in next studies. In case of the formation of low solubility products like hydroxyapatite, bioactive behaviour of magnesium may produce troubles in other applications than bone formation.

Conflict of interest

None.

Acknowledgements

We thank gratefully Regensburg Center of Biomedical Engineering (RCBE) for the support by μ -CT facility, and we acknowledge the support from the Deutsche Forschungsgemeinschaft (DFG) in frame of the program "Forschungsgeräte" (INST 102/11 – 1 FUGG).

References:

- [1] R. Dimitriou, G.I. Mataliotakis, G.M. Calori, P.V. Giannoudis, *BMC Med.* 10 (2012) 81.
- [2] R.P. Meinig, *Orthop. Clin. North Am.* 41 (1) (2010) 39–47.
- [3] G. Greenstein, B. Greenstein, J. Cavallaro, D. Tarnow, *J. Periodontol.* 80 (2) (2009) 175–189.
- [4] Y.F. Zheng, X.N. Gu, F. Witte, *Mater. Sci. Eng. R77* (2014) 1–34.
- [5] H. Hermawan, D. Dubé, D. Mantovani, *Acta Biomater.* 6 (2010) 1693–1697.
- [6] E. Willbold, A. Weizbauer, A. Loos, J.-M. Seitz, N. Angrisani, H. Windhagen, J. Reifenrath, *J. Biomed. Mater. Res. A* 105 (1) (2017) 329–347.
- [7] N.G. Grün, P. Holweg, S. Tangl, J. Eichler, L. Berger, J.J.P. van den Beucken, J.F. Löffler, T. Klestil, A.M. Weinberg, *Acta Biomater.* 78 (2018) 378–386.
- [8] T. Kokubo, H. Takadama, *Biomaterials* 27 (2006) 2907–2915.
- [9] F. Witte, J. Fischer, J. Nellesen, H.-A. Crostack, V. Kaese, A. Pisch, F. Beckmann, H. Windhagen, *Biomaterials* 27 (2006) 1013–1018.
- [10] L. Berzina-Cimdina, N. Borodajenko, in: *Infrared Spectroscopy – Materials Science, Materials Science, Engineering and Technology*, IntechOpen Limited, London, 2012, pp. 123–148.
- [11] M.S.M. Arsad, P.M. Lee, *IPCBE* 7 (2011) 184–188.

- [12] Y. Chen, Z. Xu, C. Smith, J. Sankar, *Acta Biomater.* (2014) 4561–4573.
- [13] M. Dahms, D. Höche, N.A. Agha, F. Feyerabend, R. Willumeit-Römer, *Mater. Corros.* 69 (2018) 191–196.
- [14] J. Gonzales, R.Q. Hou, E.P.S. Nidadavolu, R. Willumeit-Römer, F. Feyerabend, *Bioact. Mater.* 3 (2018) 174–1856.
- [15] H. Hornberger, S. Virtanen, A.R. Boccaccini, *Acta Biomater.* 8 (2012) 2442–2455.
- [16] M.B. Kannan, *Surf. Coat. Technol.* 301 (2016) 36–41.
- [17] X. Li, X. Liu, S. Wu, K.W.K. Yeung, Y. Zheng, P.K. Chu, *Acta Biomater.* 45 (2016) 2–30.
- [18] M.H. Idris, H. Jafari, S.E. Harandi, M. Mishahi, S. Kolyni, *Adv. Mater. Res.* 445 (2012) 301–306.